

Molecular Dynamics Simulation Study of the Rotational and Translational Motions of Liquid Acetonitrile[†]

Yoshinori Hirata

Department of Chemistry, Faculty of Science, Kanagawa University, 2946 Tsuchiya, Hiratsuka 259-1293, Japan

Received: July 3, 2001; In Final Form: October 2, 2001

By using molecular dynamics simulation, temperature and density dependences of the power spectra of the velocity autocorrelation functions of acetonitrile have been investigated. Strong temperature dependence was observed only in the low frequencies of $\leq 30 \text{ cm}^{-1}$, where the contribution of the diffusive motion was predominant, while the density effect was observed in the whole spectral region of the low-frequency phonon modes. Not only the velocity autocorrelation functions but also the velocity and the angular velocity cross correlation functions were calculated to elucidate the liquid dynamics. The amount of the angular velocity cross correlation was smaller than that of the velocity cross correlation. Oscillations were observed for angular velocity cross correlation functions, which clearly indicate that a nonnegligible portion of the initial angular momentum of the central molecule transferred to the surrounding molecules was given back to the central molecule for some time before the eventual spread over the system. We found that the angular velocity cross correlation function between the central molecule and the molecules in the outer half of the first coordination shell is negative in the short times, which suggests that the molecules move like a pair of coupled gears. Such molecular motion may be important for the diffusion process in the liquid.

1. Introduction

A detailed knowledge of the molecular dynamics of liquids is quite important for understanding of the microscopic mechanisms of the chemical reactions in solution phase. Time correlation functions of the atoms and molecules, which provide a great deal of information on the liquid dynamics, have been investigated by many researchers.^{1,2} Analysis of the velocity autocorrelation functions (ACFs) and the power spectra obtained by the Fourier transformation of the velocity ACFs is a powerful tool for the elucidation of microscopic molecular motions and can give a connection among the experimental, theoretical, and simulation works of the liquid dynamics.

By using simulation techniques, we can easily obtain not only the ACFs but also various cross correlation functions (CCFs) between the initial movement of a central molecule and the motions of the surrounding molecules, from which a knowledge of the collective dynamic properties of the molecular system can be obtained.^{3–7} Although CCFs cannot be directly accessible from experiments, they must be important to draw a detailed picture of the liquid dynamics such as relative movements of the molecules and the chemical reaction dynamics in solution. Generally the cross correlations are small but sometimes the weak correlation is due to the cancellation of different contributions, therefore the analysis of CCFs can be quite helpful to shed light on the microscopic molecular motions. Due to the recent development of ultrafast laser spectroscopy techniques, the optical Kerr effect of liquids was extensively investigated and the frequency response functions of the optical Kerr signal were analyzed in various manners.^{8–10} It was well-known that many liquids have low-frequency phonon modes in a similar frequency region.⁹ It was reported that the frequency response functions of cumene showed drastic temperature dependence

in the frequency region below $\sim 80 \text{ cm}^{-1}$.⁸ Not only the temperature variation expressed by a change in the width of the Lorentzian component centered at 0-frequency but also the extra temperature-varying component around $30\text{--}80 \text{ cm}^{-1}$ was observed. Similar temperature dependence was observed for other liquids such as CS_2 .^{8,10}

It was claimed that the observed frequency response functions of cumene at various temperatures were well reproduced by using the model of anharmonic coupling of oscillators, of which the frequency distribution was assumed to be temperature independent and was obtained from the spectrum of the low-temperature glass.⁸ Because the stiffness of the solvent cage is considered to increase with increasing liquid density, the assumption of the temperature-independent distribution of the low-frequency phonon modes seems to be curious. Therefore by using simulation techniques, we have investigated the molecular dynamics of liquids and tried to distinguish the temperature and density effects of the power spectra.

In the previous paper we reported preliminary results of the liquid dynamics of *n*-pentane.¹¹ Because of a flexible molecular structure of *n*-pentane, the power spectra obtained from the simulation were complicated and it was not easy to treat the rotational freedom. In this paper, to see the details of the liquid dynamics, acetonitrile was chosen as a model compound. Acetonitrile is a solvent widely used for various purposes and there are a great deal of activities concerned with the molecular dynamics of the liquid in the literature.^{12–14} A simulation study should be helpful in drawing a microscopic picture of the molecular motions, such as the libration and the translational and rotational diffusions in the liquid state.

2. Method

The dynamics of acetonitrile was simulated in a cubic cell of 256 molecules. All simulations were carried out by using

[†] Part of the special issue "Noboru Mataga Festschrift".

TABLE 1: Potential Parameters of Acetonitrile (Energies are given in K, lengths are in nm, and charges are in units of the charge of the proton.)

	ϵ/k_B	σ	q
CH ₃	90.6	0.38	0.269
C	105	0.30	0.129
N	48.8	0.34	-0.398

GROMACS simulation package¹⁵ and the equation of motion was integrated with the leapfrog algorithm with a time step of about 0.5 fs.¹⁶ The usual periodic boundary conditions with minimum image convention were applied. The size of the simulation cell was varied with the density of the liquid. The system was thermostated by using a weak coupling to an external heat bath with a time constant of 0.1 ps.¹⁷ To keep the density of the liquid constant, we did not adopt the pressure coupling to the external bath. During the simulation, the pressure significantly fluctuated and the standard deviation of the pressure was larger than the average pressure. Randomization of the system was carried out at the temperature of 500 K for more than 50 ps and then the system was gradually cooled to the desired temperature during a few tens of picoseconds. After the thermalization the coordinates and the velocities of atoms were stored every 5 fs for 200 ps.

The molecule was assumed to be a rigid linear object with three interaction sites.¹⁸ The united atom model was used for the methyl group. Although it is known that the liquid properties, both static and dynamic, are well reproduced by using the six-sites model of acetonitrile,¹⁹ the three-sites model can give reasonable agreements with experiments.¹⁸ Moreover the rigid linear structure of the three-sites model makes the characterization of the rotational dynamics simple, which is consistent with our purpose.

The bond lengths and the linear structure of acetonitrile were kept by using LINCS algorithm.²⁰ Each site interacts with all sites of different molecules with Lennard-Jones and Coulomb interactions. The parameters, ϵ and σ of the Lennard-Jones 6-12 potentials and the charges on the atoms are listed in Table 1. Several force fields of the 3-sites model of acetonitrile were proposed and their comparison was found in the literature.²¹ For the Lennard-Jones interaction the GROMACS force field, which is slightly different from the one widely used for simulation studies of acetonitrile, was used in our simulation. The bond lengths of $b_{\text{Me-C}} = 0.146$ nm and $b_{\text{C-N}} = 0.117$ nm were used.¹⁸ The cut-off distance of the Lennard-Jones interaction was taken to be 10 Å. The particle-mesh Ewald summation was used for the long-range Coulomb interaction.^{22,23}

Translational diffusion coefficients estimated from the mean square displacement of the molecular center-of-mass were (5.1 ± 0.3) , (4.4 ± 0.2) , (3.5 ± 0.3) , and $(2.5 \pm 0.3) \times 10^{-5} \text{ cm}^2 \text{ s}^{-1}$ at 313, 298, 283, and 253 K, respectively, which showed good agreement with the experimental values of 5.0, 4.3, 3.5, and $2.3 \times 10^{-5} \text{ cm}^2 \text{ s}^{-1}$.²⁴ Similar values were obtained by integrating the center-of-mass velocity ACF.

3. Results and Discussion

3.1. Temperature and Density Dependences of Liquid Dynamics. Nuclear dynamics of the molecular system can be discussed by using the power spectrum of the velocity ACF. The atomic and center-of-mass velocity ACFs ($A_V(t)$) of acetonitrile are displayed in Figure 1. In these simulations, to evaluate the temperature and density effects independently, we kept the density of the liquids at a constant of 0.79 kg dm^{-3} , which is the value for the real liquid acetonitrile at 298 K under atmospheric pressure.

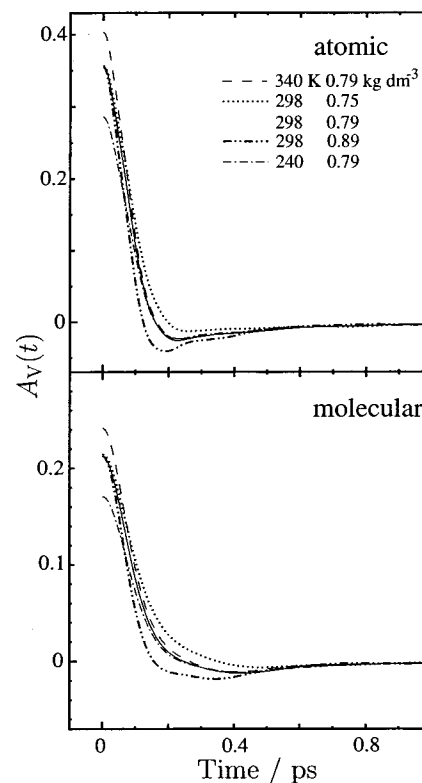


Figure 1. Temperature and density dependences of the atomic and molecular velocity ACFs of acetonitrile. Temperatures and densities are indicated in the figure.

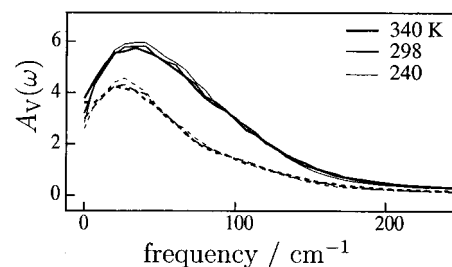


Figure 2. Temperature dependence of the power spectra of atomic (solid lines) and molecular velocity (broken lines) ACFs at 0.79 kg dm^{-3} . Temperatures are indicated in the figure.

Although $A_V(0)$, which is the mean square velocity of atoms or molecules, increased with increasing temperature, the time profile of ACFs did not show strong temperature dependence except for the long-time tailing part. On the other hand, a large density effect of the time profile was observed. The decay of $A_V(t)$ became fast and the negative correlation became significant with increasing liquid density, which indicate the increasing solvent cage effect in the high densities. To elucidate the details of the velocity ACF, power spectrum ($A_V(\omega)$) of the velocity ACF was calculated as a Fourier-cos transformation.

$$A_V(\omega) = \int_0^{\infty} A_V(t) \cos \omega t \, dt$$

The power spectrum of the atomic velocity ACF is different from either the frequency response function of the optical Kerr signal or the Raman spectrum, but it gives the frequency distribution of the molecular system and can be a reasonable representation of the density of states if the liquid is an ensemble of harmonic oscillators.²⁵

Figure 2 shows the temperature dependence of the atomic power spectra as well as the molecular power spectra, which

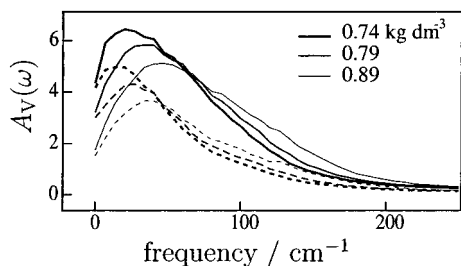


Figure 3. Density dependence of the power spectra of atomic (solid lines) and molecular (broken lines) velocity ACFs at 298 K. Densities are indicated in the figure.

were calculated from the center-of-mass velocity ACFs. For the normalization, the spectral intensities were divided by the temperatures. Since acetonitrile was assumed to be the rigid molecule and no intramolecular freedom was taken into account, only the translational and rotational motions were allowed and no significant power spectrum band was observed in the frequency region of ≥ 200 cm^{-1} .

The atomic velocity power spectrum showed a peak around 30 cm^{-1} , while the peak of the molecular velocity power spectrum was observed at ~ 25 cm^{-1} . The intensity of the power spectrum at 0-frequency, which shows the contribution of the translational diffusion, decreased with decreasing temperature. Except for the 0-frequency region temperature dependence of the spectral shape was quite weak, which suggests that the contribution of the diffusion is important for the temperature dependence of the power spectrum.

Figure 3 shows the density dependence of the atomic (solid lines) and molecular (broken lines) power spectra at the densities of 0.74, 0.79, and 0.89 kg dm^{-3} . Although the density of 0.74 kg dm^{-3} is realized at 350 K under atmospheric pressure and the density of 0.89 kg dm^{-3} is estimated to be slightly higher than that at the freezing point of acetonitrile, all the simulations were performed at 298 K. The intensity of the atomic power spectrum below ~ 70 cm^{-1} decreased with increasing density, while the intensity increased in the frequency region of > 70 cm^{-1} . The band maximum moved from ~ 20 cm^{-1} (0.74 kg dm^{-3}) to ~ 50 cm^{-1} (0.89 kg dm^{-3}). Strong density dependence was observed near the 0-frequency and the contribution of the nondiffusive oscillatory motions became important with increasing density.

A strong density dependence of the molecular power spectrum was observed in the frequency region of ≤ 50 cm^{-1} and the peak moved from ~ 15 cm^{-1} (0.74 kg dm^{-3}) to ~ 30 cm^{-1} (0.89 kg dm^{-3}). To discuss the details of the nuclear dynamics, the power spectrum of the angular velocity ACF and the difference spectrum between the atomic and molecular power spectra were compared as shown in Figure 4. These spectra are quite similar to each other except for the low-frequency region of ≤ 30 cm^{-1} . A free rotation has a constant angular momentum and appears at 0-frequency in the angular velocity power spectrum, while a velocity of the molecules oscillates at a rotational frequency, which gives a power spectrum of linear velocity at finite frequency. In the frequency region where a large difference of the angular velocity power spectrum and the difference spectrum was observed, we can expect a significant contribution of the rotational diffusion.

The results of the temperature and density dependences of the power spectra were similar to the results of our preliminary simulation study of liquid *n*-pentane,¹¹ where Coulomb interaction was not operative but a flexible structure brought various complication to the spectra. Obtaining similar results for the molecules with different characters, we may conclude that the

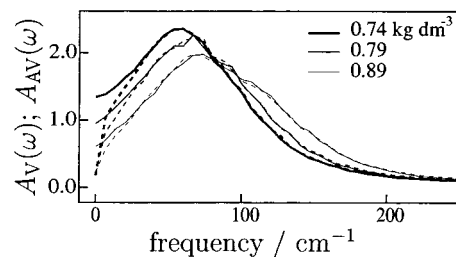


Figure 4. Density effects of the power spectra of the angular velocity ACFs (solid lines) and the difference of the atomic and molecular power spectra (broken lines) at several densities at 298 K. The intensities of the angular velocity power spectrum and the difference spectrum are normalized at the peak. Densities are indicated in the figure.

effect is quite general for various molecular systems which do not have specific intermolecular interactions such as hydrogen bonding.

The experimentally observed temperature effects of the optical Kerr effect of CS_2 and cumene appeared in a much wider frequency range than our simulation.^{8,10} Although in these experimental works the temperature and density effects cannot be distinguished from each other because the temperature and density change simultaneously, the simulation studies can give more detailed insight for these effects. Our simulation clearly shows that the power spectrum observed in the low-frequency region of ≤ 30 cm^{-1} , where diffusive motions are important, strongly depends on both the temperature and density. On the contrary, only the density effect is significant in the frequencies of ≥ 30 cm^{-1} , where libration is expected to play an important role. The experimentally observed temperature effect in the frequencies of ≥ 40 cm^{-1} should be mainly due to the density effect.

3.2. Velocity Cross Correlation Function of Liquids. To elucidate the momentum and angular momentum transfer between the molecules, we calculated the velocity and angular velocity cross correlation functions (CCFs). The velocity CCF between the central molecule (*i*) and the surrounding molecules (*j*) initially lying between the specified radii of a_n and b_n is given as

$$C_{Vn}(t) = \langle v_i(0) \cdot v_j(t) \rangle_n$$

where $\langle \dots \rangle_n$ represents a restricted statistical average. As shown in the insert of Figure 5, we calculated $C_{Vn}(t)$ for three regions: Inner and outer halves of the first coordination shell are $n = 1$ ($a_1 = 0.25$, $b_1 = 0.45$ nm) and $n = 2$ ($a_2 = 0.45$, $b_2 = 0.6$ nm), respectively, and an inner half of the second coordination shell is $n = 3$ ($a_3 = 0.6$, $b_3 = 0.8$ nm). The correlation between the atoms in the same molecule was ignored.

Figure 5a shows the atomic velocity CCFs of liquid acetonitrile at 298 K. Because of the conservation of the total momentum and the number of the particles, the velocity CCF between the central atom and all other atoms in the simulation cell should be $-A_V(t)/(N - 1)$, where N is the number of atoms in the simulation cell. A small negative value of the velocity CCF around $t = 0$ should be due to the momentum conservation during the simulation. Similar to the reported results for both the hard- and soft-sphere single-atom molecules,³⁻⁷ almost no correlation was observed at $t = 0$ and the cross correlation rapidly built up as the central atom loses its initial momentum. The peak of $C_{V1}(t)$ appeared slightly after the delay time where the first zero of $A_V(t)$ appeared. Oscillations which were reported for the velocity CCF of the mono-atomic molecules³⁻⁷ were not observed in our simulation. The decay of the $C_{V1}(t)$ should

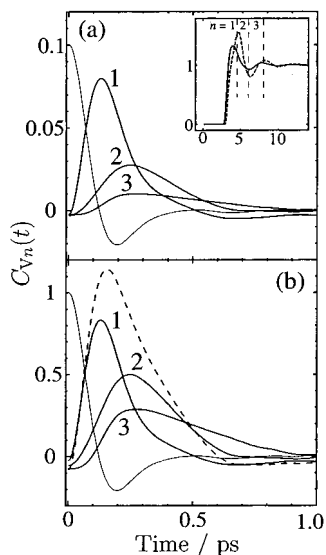


Figure 5. (a) Atomic velocity CCFs at 298 K (0.79 kg dm^{-3}) and (b) the number density weighted atomic velocity CCFs. Thin line shows the normalized velocity ACF, of which the intensity in (a) is 10 times reduced. Insert is the radial distribution function at 0.79 kg dm^{-3} . Broken line shows $C_{V_1}(t)N_1 + C_{V_2}(t)N_2$.

be due to the further momentum transfer to the atoms in the outer shell. The peak of the velocity CCF for the atoms with a larger initial separation from the central atom appeared at larger delay times. The peak of $C_{V_1}(t)$ appeared around 150 fs, while the peaks of $C_{V_2}(t)$ and $C_{V_3}(t)$ were observed around 240 and 280 fs, respectively.

$C_{V_n}(t)$ became markedly small as n increased. The amount of the momentum transfer from the central atom to the atoms in the given initial separations can be represented by $C_{V_n}(t)N_n$, where N_n is the mean number of atoms in the region n and is given by

$$N_n = 4\pi\rho \int_{a_n}^{b_n} r^2 g(r) dr$$

where ρ is the number density of the liquid.

Figure 5b shows $C_{V_n}(t)N_n$ for $n = 1-3$. The peak of $C_{V_1}(t)N_1 + C_{V_2}(t)N_2$, which is the measure of the momentum deposited in the first coordination shell, appeared at 160 fs and the peak height was slightly larger than $A_V(0)$. Thus, the results indicate that the initial momentum of the central atom was completely transferred to the atoms in the surrounding shell by this time and the diffusion of the momentum to the outer shell became significant in the longer delay times. $C_{V_3}(t)$, which represents the momentum transfer to the second coordination shell, showed a much slower decay and a smaller peak compared with those of $C_{V_1}(t)$ and $C_{V_2}(t)$.

Cross correlation functions of the center-of-mass velocity of acetonitrile are shown in Figure 6. The peaks of $C_{V_1}(t)$, $C_{V_2}(t)$, and $C_{V_3}(t)$ appeared at 130, 170, and 300 fs, respectively. The peak height of the molecular velocity CCF was much smaller than those of the atomic velocity CCF, and the peak of $C_{V_1}(t)N_1 + C_{V_2}(t)N_2$ was less than 70% of $A_V(0)$. Since the momentum transfer from the central atom to the atoms in the first coordination shell was almost unity, the initial momentum of the central molecule was converted to the freedom of other than the translational motion. In our case, the intramolecular freedom is frozen but a transfer to the rotational motion is possible. A conversion from the rotation to the translation is also possible, but in such momentum transfer no correlation measured as the molecular velocity CCF can be expected.

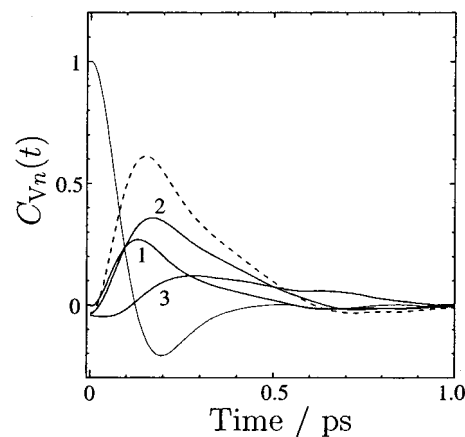


Figure 6. Molecular velocity CCFs of $n = 1, 2,$ and 3 at the density 0.79 kg dm^{-3} at 300 K. Normalized ACF is also shown in the figure. Broken line shows $C_{V_1}(t)N_1 + C_{V_2}(t)N_2$.

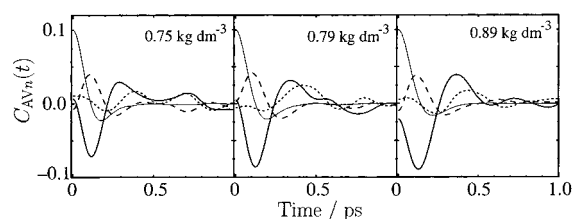


Figure 7. Density dependence of the angular velocity CCFs at 298 K. Densities are indicated in the figure. Broken, solid, and dotted lines show $n = 1, 2,$ and 3 , respectively. Normalized ACFs, of which the intensity is 10 times reduced, is also shown in the figure.

3.3. Angular Velocity Cross Correlation Function of Liquids. To see the details of the rotational dynamics, we calculated cross correlation functions of the angular velocities,

$$C_{AV_n}(t) = \langle \omega_i(0) \cdot \omega_j(t) \rangle_n$$

where $\omega_j(t)$ stands for the angular velocity of the molecule j around its center-of-mass at the time t .

Figure 7 shows $C_{AV_n}(t)N_n$ for $n = 1-3$ and $A_{AV}(t)$ at several densities. Similar to the linear velocity CCF, almost no correlation of the angular velocity was found at $t = 0$ and the rise and decay of the correlation was observed with increasing delay time. The peak intensities of the angular velocity CCFs were found to be more than 1 order of magnitude smaller than those of the linear velocity CCFs. The decays of the angular momentum CCFs were faster than those of the velocity CCFs. The delay between the peaks of molecular $C_{V_1}(t)$ and $C_{V_2}(t)$ was about 90 fs at 0.79 kg dm^{-3} (298 K), while the peaks of $C_{AV_1}(t)$ and $C_{AV_2}(t)$ appeared simultaneously. The delay between the peaks of $C_{AV_1}(t)$ and $C_{AV_2}(t)$ slightly increased with decreasing density of the liquid.

A characteristic feature of the angular velocity CCFs is the negative values of $C_{AV_2}(t)$ and the difference in signs for $n = 1$ and 2 in short delay times. If we calculate the angular velocity CCF for the whole region of the first coordination shell, CCF becomes small because of the cancellation. The results indicate that the correlation $C_{AV_2}(t)$ appeared through the direct interaction with the central molecule. The magnitude of cross correlation increased with increasing density of the liquid and the peak intensity of $C_{AV_2}(t)$ reached at the almost constant value in the densities above 0.79 kg dm^{-3} . The negative values show that molecules of $n = 2$ rotate to the opposite direction to the initial direction of the central molecule. These results suggest

that the motions of the central molecule and the molecules in $n = 2$ are similar to those of a pair of gears coupled with each other.

The peak intensity of $C_{AV3}(t)$ was much smaller than those of $C_{AV1}(t)$ and $C_{AV2}(t)$. Because of the large initial separation, direct interaction between the central molecule and the molecules of $n = 3$ seems to be negligible. The angular momentum transfer must be stepwise and $C_{AV3}(t)$ through the molecules of $n = 1$ and 2 may be canceled each other, which results in the small peak intensity of $C_{AV3}(t)$.

Oscillations were observed in the angular velocity CCFs, which suggest that nonnegligible portion of the initially transferred angular momentum to the surrounding molecules is given back to the central molecule for some time before the eventual spread over the system. The phase relation among the CCFs was not so clear as those reported for the velocity CCFs of mono-atomic molecules.⁴ The results indicate that several paths for the angular momentum transfer with different phase relations exist, which is consistent with the small peak intensities of the angular velocity CCFs. Since the peak intensity of $C_{AV2}(t)$ was rather large compared with those of $C_{AV1}(t)$ and $C_{AV3}(t)$ and the oscillation of $C_{AV2}(t)$ was clear, molecular motions similar to the coupled gear seems to be important for the diffusion process in the liquid.

4. Conclusions

Molecular dynamics simulation of acetonitrile performed in this report showed that the power spectra of velocity ACFs observed in the frequencies below 30 cm^{-1} , where the translational diffusion as well as the diffusive rotation is important, strongly depend on both the temperature and density. The contribution of the diffusive motion seems to be important for the temperature effect of the power spectra, while the density has a significant effect on both the diffusive motion and the libration.

It has been observed that the initial momentum of the central atom was completely transferred to the atoms in the surrounding shell within ~ 160 fs and the diffusion of the momentum to the outer shell became significant in the longer delay times. The amount of the momentum transferred from the central molecule to the surrounding molecules in a correlated manner was found to be less than 70% and the rest of the initial momentum of the central molecule was converted to the rotational motion.

The peak intensities of the angular velocity CCFs in the first coordination shell are more than 1 order of magnitude smaller

than those of the linear velocity CCFs, which suggests that the angular velocity transfer occurs through various paths. The most significant finding is the negative values of the angular velocity CCFs, which can be due to the molecular motions similar to a pair of coupled gears. Because of the clear oscillation of $C_{AV2}(t)$ which is the indication of the repeated angular velocity transfers between the central and the surrounding molecules. The molecular motions such as a pair of the coupled gears can be important for the diffusion process in the liquid.

References and Notes

- (1) Egelstaff, P. A. *An Introduction to the Liquid State*; Clarendon Press: Oxford, 1994, and references therein.
- (2) Balucani, U.; Zoppi, M. *Dynamics of the Liquid State*; Clarendon Press: Oxford, 1994.
- (3) Balucani, U.; Vallauri, R.; Murthy, C. S. *Phys. Lett.* **1982**, *84A*, 133.
- (4) Balucani, U.; Vallauri, R.; Gaskell, T.; Gori, M. *Phys. Lett.* **1984**, *102A*, 109.
- (5) Heyes, D. M.; Sandberg, W. C. *Phys. Chem. Liquids* **1990**, *22*, 31.
- (6) Verdaguer, A.; Padro, J. A. *J. Chem. Phys.* **1998**, *109*, 228.
- (7) Verdaguer, A.; Padro, J. A. *Phys. Rev. E* **2000**, *62*, 532.
- (8) Kinoshita, S.; Kai, Y.; Watanabe, Y. *Chem. Phys. Lett.* **1999**, *301*, 183.
- (9) Vohringer, P.; Arnett, D. C.; Westervelt, R. A.; Feldstein, M. J.; Scherer, N. F. *J. Chem. Phys.* **1995**, *102*, 4027.
- (10) Ji, X.; Ahlborn, H.; Space, B.; Moore, P. B. *J. Chem. Phys.* **2000**, *113*, 8693.
- (11) Hirata, Y. *Chem. Lett.* **2001**, 292.
- (12) Rosenthal, S. J.; Xie, X.; Du, M.; Fleming, G. R. *J. Chem. Phys.* **1991**, *95*, 4715.
- (13) Nishiyama, K.; Okada, T. *J. Phys. Chem. A* **1997**, *101*, 5729.
- (14) Maroncelli, M. *J. Chem. Phys.* **1990**, *94*, 2084.
- (15) Berendsen, H. J. C.; van der Spoel, D.; van Drunen, R. *Comput. Phys. Commun.* **1995**, *91*, 43.
- (16) Hockney, R. W. *Methods Comput. Phys.* **1970**, *9*, 136.
- (17) Berendsen, H. J. C.; Postma, J. P. M.; DiNola, A.; Haak, J. R. *J. Chem. Phys.* **1984**, *81*, 3684.
- (18) Edwards, D. M. F.; Madden, P. A.; McDonald, I. R. *Mol. Phys.* **1984**, *51*, 1141.
- (19) Bohm, H. J.; Linden-Bell, R. M.; Madden, P. A.; McDonald, I. R. *Mol. Phys.* **1984**, *51*, 761.
- (20) Hess, B.; Bekker, H.; Berendsen, H. J. C.; Fraaije, J. G. E. M. *J. Comput. Chem.* **1997**, *18*, 1463.
- (21) Mountain, R. D. *J. Chem. Phys.* **1997**, *107*, 3921.
- (22) Darden, T.; York, D.; Pedersen, L. G. *J. Chem. Phys.* **1993**, *98*, 10089.
- (23) Essmann, U.; Perera, L.; Berkowitz, M. L.; Darden, T.; Lee, H.; Pedersen, L. G. *J. Chem. Phys.* **1995**, *103*, 8577.
- (24) Hurler, R. L.; Woolf, L. A. *J. Chem. Soc., Faraday Trans. 1* **1982**, *78*, 2233.
- (25) Madden, P. A. *Liquids, Freezing and Glass Transition, Part 2*; Hansen, J. P., Levesque, D., Eds; North-Holland: Amsterdam, 1991; Chapter 7.